Amelioration of ionic conductivity (303K) with the supplement of MnO2 filler in the chitosan biopolymer electrolyte for magnesium batteries.

Adlin Helen
Christopher Selvin (csphysics@buc.edu.in)
https://orcid.org/0000-0002-3354-5790
D. Lakshmi
M.Infanta Diana

Research Article

Keywords: Biopolymer, Magnesium, battery, filler, conductivity, transference number.

Posted Date: April 21st, 2022

DOI: https://doi.org/10.21203/rs.3.rs-1557220/v1

Abstract

In the present work, the significance of adding MnO_2 filler towards development of biopolymer electrolyte, chitosan with enhanced ionic conductivity has been reported. The complexation that has taken place with the inclusion of $MgNO_3.6H_2O$ salt and MnO_2 filler in the chitosan matrix has been investigated through the Fourier Transform Infra Red (FTIR) spectra analysis. Further, the transport parameter values such as number of charge carrier densities (n), mobility (μ) and diffusion coefficient (D) have been calculated from the deconvoluted FTIR spectra. X-Ray Diffraction (XRD) and Differential Scanning Calorimetric (DSC) examination revealed that the inclusion of filler significantly reduced the degree of crystallinity and the glass transition T_g values respectively. These findings show that the inclusion of filler increases the segmental mobility of the polymer chains, allowing for faster ion transport. The conduction properties of the prepared electrolytes has been determined using Alternating Current (AC) impedance analysis, with the electrolyte containing 60 wt% magnesium salt $(2.6 \pm 0.08) \times 10^{-4}$ S cm^{-1} achieving the maximum ionic conductivity value at room temperature (303K). This value is further increased by one order of magnitude with the addition of MnO_2 filler into the polymer matrix $(1.25 \pm 0.09) \times 10^{-3}$ S cm^{-1}. To elucidate the individual contributions of ions and electrons in the conduction process, the Direct Current (DC) polarisation method has been used to determine the transference number (t_{ion}) of the produced electrolytes. The filler added chitosan polymer exhibits an extended electrochemical stability window, 1.7 V as determined by Linear Sweep Voltammetry (LSV).

1 Introduction

Lithium (Li^+) batteries have been playing a remarkable role in many applications such as energy storage grids, consumer electronic devices including mobiles, laptops, and portable chargers and most recently in Electric Vehicle (EV) transportations particularly due to its outstanding properties of high gravimetric energy density, low reduction potential, longevity and good cyclic stability [1]. This has led to an increase in demand for more lithium sources whereas some of commercially available Li^+ batteries suffer from poor thermal, chemical and mechanical stability resulting in safety issues. Few notable factors are dendrite formation, involvement of toxic and unstable chemicals, thermal stability and so on [2]. Considering these drawbacks, researchers around the world are searching arduously on finding suitable alternatives to replace and reduce the requirements for Lithium (Li^+). Along with the other post lithium ion research that includes lithium air, lithium sulphur, sodium (Na^+) and multivalent cations such as Magnesium (Mg^{2+}), Zinc (Zn^{2+}) and Calcium (Ca^{2+}) are being explored for their electrochemical properties. Among these, the multivalent cations are preferred very much since they are cost effective, less reactive in ambient temperature and most importantly available in abundance. Magnesium (Mg^{2+}) being the fifth most available element on earth is believed to be one of the most suitable alternatives to lithium (Li^+). Also the volumetric density of Mg^{2+} (3833 mAh mL^{-3}) metal is higher than Li^+ (2061 mAh mL^{-3}) metal [3]. The electro chemistries of Magnesium (Mg^{2+}) batteries are similar to Li^+ batteries but the former suffers from challenges like the lack of good compatible electrolytes with Mg^{2+} metal anode

and limited cathode availability with high specific capacity when compared to lithium electrodes [4]. While some liquid electrolytes such as grignard reagents, tetrahydrofuran (THF) etc., are quite compatible with magnesium metal anode, they undergo sluggish kinetics due to the fact that most of the multivalent cations posses high charge densities and also constitute safety risks similar to organic electrolytes of lithium batteries. On the other hand, utilizing polymer electrolytes are considered to be one of the promising approaches to overcome these challenges as they are known for properties like leakage proof, ease of fabrication, good physicochemical stability, compatibility and good interfacial contact with the electrodes. Polymer electrolytes are comparable to aqueous electrolytes in that they are made up of a polymer matrix that contains a dissociated salt [5].

Numerous works involving the investigations of synthetic polymers like poly (ethyleneoxide) (PEO), polyvinylidene difluoride (PVDF), poly (methyl methacrylate) (PMMA) have been reported for various applications including Li^+/Na^+ batteries, supercapacitors, fuel cells, actuators etc. It is reported that most of these polymers in general exhibit very poor thermal stability and conductivity at room temperature for magnesium batteries [6]. Many strategies have been reported utilizing filler and other additives such as plasticizers, ionic liquids, blending and copolymerization for enhancing the physical and electrochemical properties of the polymer electrolytes for magnesium batteries [7, 8]. Very recently Ashih Gupta and his co-workers studied the effect of 1-Ethyl-3-methylimidazolium tetrafluoroborate ($EMIMBF_4$) ionic liquid on the structural and electrochemical properties of poly (vinylidene fluoride-hexafluoropropylene) (PVDF-HFP) utilizing Mg (ClO_4) [9]. The addition of ionic liquid depressed the crystallinity in the polymer matrix thereby enhancing the ionic conductivity upto 8.3×10^{-3} S cm^{-1}. The EDLC properties of biodegradable blended polymer electrolytes based on polyvinyl alcohol (PVA) and polystyrene (PS) with magnesium acetate salt have been investigated by Sravanthi et al. [10] and when fabricated the device achieved highest power density of about 312 W/kg. Nidhi [11] and his team incorporated Al_2O_3 filler in the PVDF polymer matrix with magnesium nitrate salt and the conductivity values were increased by two orders of magnitude to 1.01×10^{-4} S cm^{-1} than the polymer without the filler. Ponraj et al. [12] reported the substantial improvement in the ionic conductivity by two orders of magnitude (10^{-5} to 10^{-3}S/cm) in triblock copolymer poly (vinylidene chloride-*co*-acrylonitrile-*co*-methyl methacrylate) (Poly (VdCl-*co*-AN-*co*-MMA)) and improved stability window with the addition of succinonitrile plasticizer. DSC and XRD analysis revealed that adding plasticizer to the polymer matrix reduced the glass transition values and increased the amorphous nature of the polymer matrix.

However the addition of toxic and flammable plasticizers or ionic liquids again highlights the concerns towards fabricating safe electrolytes for batteries and other applications. On that account ceramic inert fillers like TiO_2, ZrO_2, Ce_2O_3, ZnO, Er_2O_3, carbon based materials like graphene oxide, CNTs and active fillers like LLZO, LLTO etc. are considered to be the most reliable choice to enhance the properties of the polymer electrolytes [13]. In the case of inert fillers in polymer electrolytes, the filler plays no direct part in the ionic conduction process, as the name implies. The improvement in conductivity was found due to interactions of the surface groups of the filler particles with polymer chains and the salt [14]. These fillers have been reported to hinder crystallisation kinetics, enabling the enhancement of amorphous nature in

the polymer matrix [15]. This in turn results in the increase of the free volume as well as the mobility of the polymer segments near the filler surface. With the addition of filler to the polymer matrix, the hopping mechanism associated with polymer segmental motion is observed to be improved [16].

It is worth to be noted that the synthetic polymers mentioned above are derived from hazardous petroleum sources and pose a major environmental threat besides being very expensive [17]. In contrast, biopolymer electrolytes are biodegradable, cheap and non toxic since they are derived from natural sources that include polynucleotides, polypeptides, polysachharides and other structural macromolecules. Some examples of biopolymers are cellulose, starch, lignin, chitosan, agar-agar, pectin, gellan gum, gelatin, sodium alginate,etc. Chitosan, one of the most abundant biopolymers available is derived from deactylation of chitin, a polysachharide present in the crab shell which is also a biowaste and is being investigated widely for its excellent properties, especially in applications like water purification, drug delivery, biosensors, actuators, supercapacitors etc. [18, 19] and therefore, it has been chosen as the host matrix in the present work. When inorganic salts of lithium, magnesium, sodium, calcium, and other metal cations and anions are dispersed into the matrix, the presence of electrons in the characteristic amine and hydroxyl groups of chitosan facilitates the formation of bonds with those metal cations and anions. This is considered to be one of the important prerequisites for a polymer electrolyte to dissociate the salt into ions which in turn affects the structural, thermal and electrochemical properties of the polymer [20].

Magnesium nitrate hexahydrate ($MgNO_3.6H_2O$) has been selected as the magnesium salt of choice for ionic conduction (Mg^{2+}) and MnO_2 as the inert filler for enhancing the conductivity properties for the preparation of chitosan biopolymer electrolytes in this work. MnO_2 one of the widely used metal oxides with very good physical and chemical properties has been used in variety of applications such as biosensors, biocatalysts and as electrodes in energy storage devices [21,22]. Yuhan Li et al. studied the enhanced Li^+ ion transport (1.5 times higher) along with reinforced mechanical strength (2.3 times better tensile strength) upon the addition of filler MnO_2 nanosheet than the pure PEO lithium salt complexes [23]. Similarly Say Min Tan and his team reported the increment of ionic conductivity ($5.79x10^{-3}$ S/cm) with the addition of MnO_2 in the PMMA-PEO-$LiClO_4$ polymer electrolyte plasticized with ethylene carbonate (EC) [24]. As per the literature survey, no works have been reported on developing magnesium conducting chitosan biopolymer electrolyte incorporating MnO_2 filler. On account of this, the effectiveness of using MnO_2 filler in increasing the conductivity and other properties of magnesium conducting biopolymer electrolytes based on chitosan, prepared with $MgNO_3.6H_2O$ salt have been investigated and the results are stated.

2 Experimental

2.1 Materials Used

Chitosan biopolymer (75% deacetylated chitin) has been procured from LOBA chemicals, glacial acetic acid (99% purity) from Himedia, Magnesium nitrate hexahydrate ($MgNO_3.6H_2O$) from Himedia, and Manganese dioxide (MnO_2) from SRL chemicals.

2.2 Synthesis procedure

The solid polymer electrolytes are prepared with the appropriate amount of Chitosan biopolymer dissolved in 100ml of 1wt% acetic acid solution with different weight percentages of $MgNO_3.6H_2O$ salt added to it. The polymer–salt solution is allowed to stir till it becomes homogenous and desired viscosity is obtained. The resultant viscous solutions are then cast on the petri dishes and are made to dry at room temperature. The salt added polymer electrolytes are named as CN50, CN60, CN70 and CN80 according to the amount of salts added in weight percentages (50, 60, 70 and 80 wt %). Similar procedure is followed to synthesize polymer electrolytes with MnO_2 filler in various amounts (0.5, 1, 2 and 3 wt %) and the samples are named as such: C0.5Mn, C1Mn, C2Mn and C3Mn.

2.3 Characterization methods

The XRD analysis of the prepared polymer electrolyte samples have been carried out with the help of panalytical X'PERT-PRO diffractometer using CuKα source. The changes in the vibrational peak intensity of the functional groups present in the polymer host on adding the salt and MnO_2 filler have been analysed using FTIR (MIRacle 10-ZnSe) instrument. The glass transition temperature (T_g) has been found using DSC analysis (Netzsch) and the weight loss percentage occurred while subjecting the samples to various range of temperature in N_2 atmosphere is found using Thermo Gravimetric analysis instrument (EXSTAR/6300). The electrochemical properties like measurement of room temperature ionic conductivity and voltage stability have been investigated through impedance analysis and Linear Sweep Voltammetry (LSV) analysis (Biologic SP 300 workstation in the frequency range 10Hz to 1MHz and in the voltage range 0 to 3V) respectively. The room temperature transference numbers (t_{ion}) have been measured using DC polarization method in the symmetric SS/PE/SS (SS-Stainless Steel) electrode configuration with the voltage supply of 1V.

3 Results And Discussion

3.1 Functional Group Analysis

The evidence of functional groups present in the prepared polymer electrolytes have been confirmed using FTIR analysis. Figure 1 shows the FTIR spectra of $MgNO_3.6H_2O$ salt and MnO_2 filler. Through the changes observed in the vibrational peak intensities and shift in wave numbers from the Fig. 2, the formation of complex between the polymer host, salt and the filler has been confirmed. The characteristic vibrational peaks observed around 3360 cm^{-1}, 1550 cm^{-1}, 1360 cm^{-1}, 800 cm^{-1} and 670 cm^{-1} are ascribed to = OH stretching, □ O bending, N □ O asymmetric stretching(v_3), NO^{3-} deformation and MgO peaks (metal oxygen) respectively of $MgNO_3.6H_2O$ salt [25]. Figure 2 displays the FTIR spectra of the

pure chitosan and chitosan with different weight percentages of salt. With the addition of salt, the intensity of the characteristic peaks of chitosan seen at 3389 cm^{-1} due to O–H stretching groups is found to be reduced and expanded, indicating improved hydrophobicity of the chosen polymer electrolyte. The vibrational peaks at 2978 cm^{-1} assigned to –CH symmetric and asymmetric vibrations of typical polysachaaride have been disappeared on adding the salt. This disappearance of peaks indicates the dissociation of salt into ions thereby forming complex with the polymer chains via –H bonding [26]. The further notable peaks at 1558 cm^{-1}, 1651 cm^{-1} and 1072 cm^{-1} corresponds to symmetric deformation of NH_3^+ (amine II) groups, O = C NH stretching (carbonyl amide I) and strong C–O–C vibrations respectively of the chitosan biopolymer [27].

<Fig. 1**>**

The shift in the C–N stretching (amideII) vibrational peaks from 1387 cm^{-1} to 1379 cm^{-1} assures the inter - molecular interaction of the polymer matrix with the anion of the salt. According to Rahman et al. this could be due to the weakening of the interaction or an increase in bond length between the cation and the amine group, both of which would play an important role in ionic mobility when an electric signal is supplied [28]. The changes in intensities found at 671 cm^{-1} indicates the coordinate complex formation between the Mg^{2+} cation with twisting $–NH_2$ vibrational groups with lone pair of electrons ($NH_2....Mg^{2+}$) [29].

<Fig. 2**>**

Further from the Fig. 1 the vibrational peaks of MnO_2 found at 1694 cm^{-1}, 1533 cm^{-1}, 1385 cm^{-1}, 987 cm^{-1} corresponds to –OH bending vibrations complexed with Mn atoms and those around 684 cm^{-1} and 596 cm^{-1} belongs to stretching Mn–O bonds present within the MnO_2 structure [30] and the changes observed with the addition of MnO_2 to the polymer electrolyte with 60 wt% salt (CN60) is given in Fig. 3. It should be noticed that while there are no symmetrical changes with the addition of filler, the intensities of the vibrational peaks are much reduced as the filler content is increased. This suggests that the inclusion of filler has a considerable impact on the amorphous nature polymer electrolytes, which is consistent with the results of the XRD analysis presented in the next section. According to the literature, this is due to the lewis acid-base like interactions of MnO_2 filler with electron rich NH_2, oxygen and hydroxyl characteristic groups of the chitosan and also with the ions in the dopant salt in which the cations acts as lewis acid centre and anions as lewis base centre. These interactions lead to the development of free volume inside the polymer matrix, resulting in a more efficient kinetic pathway for ion migration [31].

<Fig. 3**>**

3.1.1 Analysis of transport parameters from FTIR absorption spectra

The transport properties of ions present in the prepared polymer electrolytes before and after the addition of filler are evaluated by deconvolution of FTIR spectra in absorption mode. The vibrational peak range where changes in peak intensity, shift in wavenumbers observed is usually selected for deconvolution and the deconvoluted FTIR responses are presented in Supplementary Information (Fig. S1). Here the deconvolution is carried out for the vibrational peaks in the frequency range between 1500 cm^{-1} and 1200 cm^{-1} belonging to the characteristic peaks of NH_3^+ (amine II) of the polymer (around 1389 cm^{-1}) where a shift to lower wavenumbers due to complexation with anion group (NO_3) in the salt belonging to N–O symmetric stretching vibrations of the ionic salt is observed. The percentage of free ions and ion aggregates present in the polymer matrix are calculated using the following Eq. (1):

$$\text{Percentage of free ion (\%)} = \frac{Area of free ions peak}{Total area\,(free ions peak + ion pairs peak)} \text{ x } 100\% \quad (1)$$

The calculated values are given in Table 1. It is found that the highest percentage of free ions is found for the electrolyte with 60 wt% of $MgNO_3.6H_2O$ salt (CN60) and this value is reduced with increase in salt concentration above 60wt%. This confirms the formation of ion pairs or ion agglomerates at increasing concentrations of salt. The percentage of free ions in the electrolyte CN60, on the other hand, is observed to be increased when filler is added. This shows that adding the filler causes the salt to dissociate into a greater number of free ions, which could be correlated to the contributory factor in improved ionic conductivity of these polymer electrolytes [32]. Again, this value is decreased on adding MnO_2filler more than 2 wt% indicating that the capacity of the polymer matrix to accommodate the filler particles has reached a threshold, and adding more filler reduces the distance between each ion, resulting in ion agglomeration of filler particles.

Table 1
Free ion percentage, number of charge carriers (n), mobility (μ) and diffusion coefficient (D) for the prepared polymer electrolytes with variation in salt and filler content

Sample	Free ion (%)	$n(cm^{-3}) \times 10^{22}$	$\mu(cm^2v^{-1}s^{-1}) \times 10^{-10}$	$D(cm^2s^{-1}) \times 10^{-11}$
Chitosan + salt				
CN50	40.5	2.3	0.4	1.0
CN60	63.4	5.5	2.9	6.8
CN70	34.4	4.7	1.9	4.4
CN80	11.5	2.5	1.7	4.0
CN60 + MnO_2				
C0.5Mn	64	5.5	0.4	0.8
C1Mn	64.9	5.6	0.3	0.9
C2Mn	70	6.1	1.3	3.0
C3Mn	35.5	3	0.6	1.4

To support this further, the transport properties such as ionic mobility (μ), number of charge density (n) and diffusion coefficient (D) values have been calculated using the free ion percentage values employing the following Eqs. 2, 3 and 4:

$$n = \frac{M \times N_A}{V_{total}} \times (freeion\%)$$

2

$$\mu = \frac{\sigma}{ne}$$

3

$$D = \frac{\mu kT}{e}$$

4

where M is the number of moles of salt, N_A is the avagadro's number, V_{total} is the volume of the polymer electrolytes (cm^3), σ is the ionic conductivity measured from AC impedance analysis (S cm^{-1}), n is the

number of charge carriers, e is the electronic charge (1.6 x 10^{-19} C), k is the Boltzman constant (1.38 x 10^{-23} J K^{-1}) and T is the temperature in Kelvin (K) [33]. It is found that the values of these transport parameters obtained as presented in Table 1 are in proportion with the trend observed in the ionic conductivity values (Table 3) obtained for the electrolytes. The values of these transport parameters obtained are increased till 60 wt% of salt in the polymer electrolytes (CN60), after which there is a sudden decline in the values. However these values are increased with the addition of filler in the CN60 polymer electrolytes. As previously noted in the FTIR spectra analysis, the interaction of filler groups with the ions in the salt results in enhancing the dissociation of salt into a considerable number of free ions which also leads to creation of free space inside the polymer matrix, allowing the ions to migrate more easily and could be correlated to the increase in the transport parameter values.

<Table 1**>**

3.1.2 Possible Conduction mechanism

The probable interaction that could have happened between the salt, filler, and characteristic groups present in the chitosan polymer matrix has been illustrated in Scheme 1 based on the changes found in the vibrational bands from the FTIR analysis. The Mg^{2+} cation forms complexes with the electron-rich groups in the polymer backbone, whereas the anion interacts with the carbonyl groups (Scheme 1a). The ion-ion interaction happens when the polymer matrix has exceeded its saturation point for accommodating the ions, resulting in the formation of ion pairs at higher salt concentrations as evident from the calculated free ion values.

<Scheme 1>

On adding MnO_2 filler to the polymer electrolyte CN60 (Scheme 1b), the cations and anions of the salt begin to interact with the surface groups of the MnO_2 filler (filler-ion interaction). Also, the fillers serve as cross linking centres with the characteristic groups present in the polymer segment (filler-polymer interaction). This is expected to result in the increase of the free space within the polymer matrix, facilitating the movement of ions from one coordinated site to another.

3.2 Structural Analysis

Figure 4 shows the XRD diffractograms of the prepared chitosan biopolymer electrolytes with various wt % of $MgNO_3.6H_2O$ salt. The characteristic peaks observed at 15.3 °, 20° and 30 ° indicate the semicrystalline nature of the pure chitosan [34]. It should be noted that the addition of salt causes the intensity of the diffracted peaks of the chitosan polymer host to be uplifted. According to Faisal I Chaudry et al. this is due to the interaction of ions in the salt with functional groups existing in the polymer host, such as NH_2 with the lone pair of electrons, as well as other oxygen and hydroxyl groups, and this has been validated by FTIR analysis [35]. However the intensity is found to be low for the polymer electrolyte with 60 wt % of $MgNO_3.6H_2O$ salt when compared to other salt added polymer electrolytes and the crystalline nature is found to be increased again at higher concentrations of salt. Also the degrees of

crystallinity values are increased initially with the addition of salt. This is in alignment with glass transition values (T_g) obtained from DSC analysis.

<Fig. 4>

It is to be noted that the intensity of the characteristic diffracted peak of CN60 is reduced extensively with incorporation of MnO_2 filler to the polymer host (CN60) as evident from the Fig. 5. Also this is in agreement with the degree of crystallinity (χ) values obtained using the Eq. 5 and the calculated values are given in Table 2.

Table 2
Degree of crystallinity values calculated for the prepared electrolytes

Sample	Degree of Crystallinity (± 0.1)
Chitosan + salt	
Pure Chitosan	15.6
CN50	20.5
CN60	16.4
CN70	21.3
CN80	21.8
CN60 + MnO_2	
C0.5Mn	12.1
C1Mn	11.2
C2Mn	8.1
C3Mn	8.9

$$\chi = \frac{Area of crystalline peaks}{Total area\,(Amorphous + Crystalline)} x(100\%) \quad (5)$$

This decrease in peak intensity is owing to the addition of filler, which confirms the suppression of recrystallization in the polymer matrix, resulting in an increase in the amorphous phase [36]. This also indicates the increase in free volume inside the host matrix, giving rise to more conduction pathways for free ion mobility. The polymer electrolyte with 2 wt% of filler has shown lowest degree of crystallinity values. However this value is found to be increased on increasing the filler content above 2 wt%. This rise in crystallinity might be attributed to the creation of ion pairs or ion aggregates inside the polymer matrix, based on the percentage of free ion values determined using deconvolution of FTIR spectra. Furthermore, the absence of any distinct peaks of both salt and filler in the diffractograms obtained for the prepared

electrolytes indicates that salt and filler have completely dissociated in the polymer matrix, confirming the interaction that has occurred in the polymer matrix among the characteristic groups with the salt and filler.

<Fig. 5**>**

<Table 2**>**

3.3 DSC and TG Analysis

The DSC thermograms exhibiting endothermic peaks for all the prepared polymer electrolytes are given in Fig. 6. The T_g value of pure chitosan observed around 53 °C is found from Fig. 6a. This T_g value has been found to be increased initially to 60 °C on adding the salt (Fig. 6b). The ion-dipole interaction between the electron rich groups in the polymer and the ions in the salt causes the segmental polymer chain dynamics to be reduced, resulting in an increase in T_g value [37]. However, when the salt content is increased to 60%, the T_g value drops, indicating that crystallisation is reduced and confirming the development of transitory cross linkages between the salt and the functional groups present in the polymer matrix, stiffening the polymer. However, as the salt concentration is increased above 60%, the T_g value increases again, which could be due to the agglomeration of ionic clusters of salt groups, which reduces the segmental mobility of the polymer chains. This is also consistent with the crystallinity degree values obtained from XRD diffractograms. It is worth noting that adding MnO_2 filler to polymer CN60 reduced the glass transition temperature (T_g), indicating that changes happened in the amorphous regions of the prepared polymer electrolytes, making the electrolytes more flexible (Fig. 6c). According to Benson K Money et al. this decrease in T_g after adding the filler, confirms the interaction of filler groups with polymer-salt complexes, which accelerates polymer chain dynamics [38]. Increasing the filler content above 2 wt% reduces the T_g value again. The lowest T_g value obtained for polymer with 2 wt% filler is expected to achieve the highest ionic conductivity, which is due to the dipole orientation of filler groups while interacting with polymer functional groups and the salt, resulting in an increase in the amorphous phase inside the matrix, as explained in FTIR analysis. The TG analysis has been performed to examine the reduction in the weight loss percentages of the polymer electrolytes with the addition of filler, as shown in Fig. 7. The evaporation of water solvent is primarily accountable for the weight loss observed in all samples at two phases. The inclusion of filler has clearly improved the weight loss percentage to a reasonable proportion, as evidenced by the thermograms. This implies that the filler particles present inside the polymer matrix inhibits the evaporation of solvent and water content in the electrolytes denoting the improvement in the thermal stability [39].

<Fig. 6**>**

<Fig. 7**>**

3.4 Impedance Analysis

The ionic conductivity measurement at room temperature (303 K) has been carried out using impedance analysis and the nyquist plots with the corresponding equivalent circuits of the pure chitosan, chitosan with different weight percentages of $MgNO_3.6H_2O$ salt are displayed. For pure chitosan, a depressed semicircle with high bulk resistance (R_b) is obtained (Fig. 8a). However on adding different weight percentages of salt to the pure chitosan matrix, the value of R_b is decreased as seen from the nyquist plots (Fig. 8b) exhibiting two depressed semicircles for the salt added polymer electrolytes. The electrochemical behaviour observed at both the semicircles are represented by the parallel combination of resistance and CPE and the relevant equivalent circuit is given in the Fig. 8b. The conductivity values are calculated using the Eq. 6,

$$\sigma = \frac{t}{R_b A}$$

6

Where t is the thickness of the electrolytes samples, R_b is the bulk resistance and A is the area of the electrolyte. The first semicircle obtained in the high frequency region corresponds to parallel combination of bulk resistance (R_b) and the capacitance (non ideal) whereas the second semicircle in low frequency region corresponds to charge transfer resistance (R_{ct}) and double layer capacitance at the blocking electrode interface [40].

<Fig. 8**>**

A maximum conductivity of about $2.6x10^{-4}$ S cm^{-1} is found in chitosan biopolymer electrolyte with 60 wt% salt (CN60), as expected by DSC and XRD studies. The conductivity values are also found to be declining as the salt concentration is increased over this threshold value of 60 wt%. This decrease in ionic conductivity, according to Koduru et al. is due to the strong columbic attraction that exists between the ions at high salt concentrations, resulting in the creation of ionic salt clusters, as validated by FTIR deconvolution analysis. This in turn hinders the charge carrier transport within the polymer matrix [41]. Figure 8c shows the nyquist plots of the polymer electrolytes with 60 wt% salt and various amounts of MnO_2 filler (0.5 to 3 wt %). Similar to salt dispersed chitosan biopolymer electrolytes two depressed semicircles are observed whereas the diameter of these semicircles has been reduced extensively that resulted in the augmentation of ionic conductivity values and for the electrolyte with 2 wt% of filler C2Mn achieving the highest value by an increase of one order of magnitude ($1.25x10^{-3}$ S cm^{-1}). This is due to the fact that the crystalline phase in the salt dispersed chitosan polymer matrix is disrupted with the addition of MnO_2 filler, and similar observations have been reported in the literature [42]. This is also in consistent with the decrease in degree of crystallinity and T_g values obtained from XRD and DSC analysis, which further confirms the decrease in the tendency of polymer chains to reorganise due to weakening of coordinative bonds between cations and electron rich groups in polymer with the addition of filler. Also the increment in the ionic conductivity values is supported with the increase in number of charge carrier values and other transport parameters like ionic mobility (μ) and the diffusion coefficient

(D) obtained using the free ion percentage values calculated from the deconvolution of FTIR spectra. Due to the influence of local dielectric environment or space charge polarisation of the filler, the inclusion of the filler enhances the dissociation of magnesium salts into more number of free charge carriers [43]. The increase in trend with ionic conductivities with respect to both salt and filler content separately is given in Table 3 and the corresponding circuit parameter values are presented in Supplementary Information (Table S1)

Table 3 Conductivity (σ) and Resistance(R) values of the prepared electrolytes.

Sample Code	σ (S cm^{-1})
Chitosan+salt (± 0.08)	
Pure Chitosan	6.3×10^{-9}
CN50	1.7×10^{-5}
CN60	2.6×10^{-4}
CN70	1.05×10^{-4}
CN80	7.18×10^{-5}
CN60+MnO_2 (±0.09)	
C0.5Mn	3.33×10^{-4}
C1Mn	3.12×10^{-4}
C2Mn	1.25×10^{-3}
C3Mn	2.84×10^{-4}

<Table 3**>**

However a decline in ionic conductivity value is seen while increasing the filler content above 2wt%. This implies that the threshold limit of the polymer electrolyte in accommodating filler particles is 2wt%, and that adding more filler particles will only result in the creation of filler clusters, which will prevent charge carriers from moving freely through the interfacial pathway. Many similar works reported related to significant effect in enhancing the ionic conductivity with the addition of fillers in polymer electrolytes given in Table 4.

Table 4
List of polymer electrolytes with filler and their conductivities.

Polymer	Filler	Ionic salt	Conductivity hike (S cm^{-1})	Reference
PEO	ZrO_2	$NaPF_6$	5×10^{-8} to 3×10^{-6}	44
Corn starch	Al_2O_3	LI	1×10^{-4} to 6×10^{-4}	45
Starch/chitosan	GO	$LiClO_4$	9×10^{-6} to 3×10^{-3}	46
CS/CMC	CNT	$LiClO_4$	1×10^{-4} to 3×10^{-3}	47
Chitosan	ZrO_2	$LiClO_4$	2×10^{-5} to 3×10^{-4}	48
Chitosan	V_2O_5	$MgCl_2$	4×10^{-4} to 1×10^{-3}	49
Chitosan	MnO_2	$MgNO_3.6H_2O$	2×10^{-4} to 1×10^{-3}	Present work

<Table 4**>**

3.5 Transference Number

The transference number (t_{ion}) helps in confirming the ionic contribution of the polymer electrolytes in the conduction process. The charge carried by the ions to the total charge carried by both the ions and the electrons present in the sample gives the transference number (t_{ion}). The transient current (I) observed while subjecting the polymer electrolytes to a voltage of 1 V and the corresponding decrease in current (I) over the time (in hours) is given in the Fig. 9a and Fig. 9b. The drop in steady state current (I) shows complete dissociation of ionic species inside the polymer matrix, with the electronic contribution accounting for the remaining current [50].

<Fig. 9**>**

With the help of the current (I) values obtained at the final and initial stages of polarization, the transference number (t_{ion}) values have been calculated employing the following Eq. 7,

$$t_{ion} = \frac{I_i - I_s}{I_i} \quad (7)$$

where I_i and I_s represents the initial and the steady(final) state current respectively. The transference number (t_{ion}) is found to be higher for the polymer electrolyte with 2wt% of MnO_2 filler (C2Mn) which could be correlated to the increase in charge carriers or free ion percentage on dispersing the filler into the polymer matrix [51]. With the help of the transference number (t_{ion}) obtained, the individual contribution of cations and anions in the transport parameters diffusion coefficient (D) and mobility (μ), can be substantiated using the following Eqs. 8, 9, 10 and 11:

$D = D_+ + D_- = \frac{KT\sigma}{ne^2}$ (8)

$t_{ion} = \frac{D_-}{D_+ - D_-} = D_+/D$ (9)

$\mu = \mu_+ + \mu_- = \frac{\sigma}{nq}$ (10)

$t_{ion} = \frac{\mu_+}{\mu_+ + \mu_-}$ (11)

D+, D-, μ_+ and μ_- denote the contribution of cations and anions in diffusion process (D) and mobility (μ) respectively. It is obvious from the Fig. 10 that the contribution of cations in both the diffusion coefficient and mobility is found to be higher in C2Mn than the polymer electrolyte without the filler CN60. Thus it is confirmed that the majority charge carriers are Mg^{2+} cations and could be considered for its employment in the magnesium batteries [52].

<Fig. 10**>**

3.6 Stability window analysis

Figure 11 displays voltammograms of the electrolytes CN60 and C2Mn carried out against stainless steel (SS) electrodes using LSV analysis. LSV helps to validate the improvement in the electrochemical voltage window of the highest salt conducting polymer electrolyte (CN60) with addition of 2wt% of MnO_2 (C2Mn). It is found that the stability window has been increased from 1.4 V to 1.7 V on adding MnO_2 filler. In addition, a prototype of primary magnesium battery with the highest conducting polymer electrolyte (C2Mn) has been fabricated and is given in Supplementary Information (Fig. S2) along with the observed Open Circuit Potential (OCP) and discharge profile characteristics (Fig. S3).

<Fig. 11>

4 Conclusion

Thus, based on the obtained results, the significance of dispersing MnO_2 filler in increasing the ionic conductivity has been substantiated in the chitosan biopolymer electrolyte prepared with $MgNO_3.6H_2O$ salt. Consequently, the highest conductivity is achieved by one order of magnitude (1.25 ± 0.09) x 10^{-3} Scm^{-1}) in the sample with 2 wt% of MnO_2 .This is supported with the results obtained from XRD, DSC, TGA and FTIR analysis. The reduction in degree of crystallinity and glass transition temperature (T_g) values with the addition of MnO_2 filler, as evidenced by XRD and DSC results, indicates the creation of more free volume inside the polymer matrix along with an increase in number of charge carrier densities (n), ionic mobility (μ), and diffusion coefficient (D) values calculated from FTIR deconvolution analysis in absorption mode. These observations show that adding MnO_2 to the salt dissociated it into a significant number of free ions, inhibiting ion aggregation formation. The presence of ionic behaviour in the

produced electrolytes has been further confirmed by the transference number analysis (t_{ion}). The electrochemical stability window extended to 1.7 V on the addition of MnO_2 filler in chitosan matrix, indicating the hopeful choice of the polymer electrolyte for device application.

Declarations

Funding

The authors declare that no funds have been received during the preparation of manuscript.

Conflict of interest

The authors have not disclosed any conflicts.

Author Contributions

Conceptualization, Methodology, Formal analysis and investigation, writing-original draft preparation: [P.Adlin Helen], Supervision: [Dr.P.Christopher Selvin], Review and editing: [D.Lakshmi], [M.Infanta Diana]

References

1. Y. Liu, Z. Sun, D.K. Denis, J. Sun, L. Liang, H. Linrui, Y. Changzhou, J. Mater. Chem. A (7), 4353 (2019)
2. A. Manthiram, X. Yu, S. Wang, Nat. Rev. Mater. **2**, 16103 (2017)
3. J. Yang, H. Zhang, Q. Zhou, H. Qu, T. Dong, M. Zhang, B. Tang, J. Zhang, G. Cui, ACS Appl. Mater. Interfaces **11**, 17109 (2019) (**19**
4. M. Asif, S. Kilian, M. Rashad, Energy Storage Mater. **42**, 129 (2021). https://doi.org/10.1016/j.ensm.2021.07.031
5. M.C. Long, T. Wang, P.H. Duan, Y. Gao, X.L. Wang, G. Wu, Y.Z. Wang, J. Energy Chem. **65**, 18 (2022). https://doi.org/10.1016/j.jechem.2021.05.027
6. P. Chen, Q. Zheng, Q. Li, R. Zhao, Z. Li, X. Wen, W. Wen, Y. Liu, A. Chen, Z. Li, X.Liu Chem. Eng. J **427**, 132025 (2022)
7. Z. Liu, X. Wang, Z. Liu, S. Zhang, Z. Lv, Y. Cui, L. Du, K. Li, G. Zhang, M.C. Lin, H. Du, ACS Appl. Mater. Interfaces **13**(24), 28164 (2021)
8. L. Gao, J. Li, J. Ju, B. Cheng, W. Kang, N.Deng Compos. Sci. Technol. **200**, 108408 (2020)
9. A. Gupta, A. Jain, S.K.Tripathi Polym. Res. **28**, 235 (2021). https://doi.org/10.1007/s10965-021-02597-9
10. K. Sravanthi, G.S. Sundari, H. Erothu Optik **241**, 166229 (2021)
11. S.Patel,R.KumarMater.Today:Proc462175(2021)https://doi.org/10.1016/j.matpr.2021.02.691
12. T.Ponraj,.Srikumar, A.Ramalingam,S.Selvasekarapandian,S.R. R.Manjuladevi Polym.Bull. **78**, 35 (2021)

13. J. Cheng, G. Hou, Q. Chen, D. Li, K. Li, Q. Yuan, J. Wang, L. Ci Chem. Eng. J. **429**, 132343 (2022)
14. P. Cui, Q. Zhang, C. Sun, J. Gu, M. Shu, J. Gu, M. Shu, C. Gao, Q. Zhang, W. Wei RSC Adv **12**, 3837 (2022)
15. D.E. Mathew, S. Gopi, M. Kathiresan, A.M. Stephan, S. Thomas Electrochim. Acta **319**, 189 (2019)
16. G.Zang,M.He,Y.Liao,M.Li,M.Hong,W.Li,Ionics 28, 767(2022)https://doi.org/10.1007/s11581-021-04351-z
17. M. Rayung, M.M. Aung, S.C. Azhar, L.C. Adsullah, M.S. Su'ait, A. Ahmad, S.N. Jaamil Materials **13**(4), 838 (2020). https://doi.org/10.3390/ma13040838
18. B.K. Roy, I. Tahmid, T.U. Rashid, J. Mater. Chem. A **9**, 17592 (2021)
19. P.K. Panda, P. Dash, J.M. Yang, Y.H. Chang Cellulose **29**, 2399 (2022). https://doi.org/10.1007/s10570-021-04348-x
20. R. Alves, R.C. Sabadini, T.S. Gonçalves, A.S.S. De Camargo, A. Pawlicka, M.M. Silva.Int, J. Green. Energy **16**(15), 1602 (2019)
21. L. W.Sun, Y. Chen, Y. Wang, ,S. Zhou, Meng, H.Li ,Y., Luo, Synth, React. Inorg. Met. -Org Chem. **46 (3)**, 437 (2016). https://doi.org/10.1080/15533174.2014.988250
22. M.R. Johan, L.M. Ting Int. J. Electrochem. Sci. **6**, 4737 (2011)
23. Y. Li, Z. Sun, D. Liu, Y. Gao, Y. Wang, H. Bu, M. Li, Y. Zhang, G. Gao, S. Ding, J. Mater. Chem. A **8**, 2021 (2020)
24. S.M. Tan, SM, M.R. Johan Ionics **17**, 485 (2011). https://doi.org/10.1007/s11581-011-0541-7
25. M. Sulaiman, A.A. Rahman, N.S. Mohamed Int. J. Electrochem. Sci. **8**, 6647 (2013)
26. N.M. Khan, N.F. Mazuki, A.S. Samsudin, J. Electron. Mater. **51**, 745 (2022). https://doi.org/10.1007/s11664-021-09372-y
27. A. Poosapati, K. Negrete, M. Thorpe, J. Hutchison, M. Zupan, Y. Lan, D. Madan, J. Appl. Polym. Sci. **138**(33), 50813 (2021)
28. N.A. Rahman, S. Navaratnam, S.Z. Abidin, F.A. Latif, A.I.P. Conf. Proc. 2020 (1) 020076 (2018) https://doi.org/10.1063/1.5062702
29. S. Majumdar, P. Sen, R. Ray, Mater. Today: Proc. **18** 4913 (2019) https://doi.org/10.1016/j.matpr.2019.07.483
30. M. Mylarappa, V.V. Lakshmi, K.V. Mahesh, H.P. Nagaswarupa, N. Raghavendra IOP Conf. Ser. : Mater. Sci. Eng. 149 (2016) https://doi.org/10.1088/1757-899X/149/1/012178
31. A.C. Nancy, S.A. Suthanthiraraj, Ionics 23, 1439 (2017). https://doi.org/10.1007/s11581-017-1976-2
32. N.A. Shamsuri, S.N. Zaine, Y.M. Yusof, W.Z. Yahya, M.F. Shukur, MF. Ionics **26**, 6083 (2020). https://doi.org/10.1007/s11581-020-03753-9
33. V. Sundararajan, N.M. Saidi, S. Ramesh, K. Ramesh, G. Selvaraj, C.D. Wilfred, J. Solid State Electrochem. **23**, 1179 (2019). https://doi.org/10.1007/s10008-019-04207-7

34. N.A. Rahman, S.A. Hanifah, N.N. Mobarak, A. Ahmad, N.A. Ludin, F. Bella, M.S.Su'ait Polymer **230**, 124092 (2021)
35. F.I. Chowdhury, J.Islam,A.K. Arof, M.U. Khandaker, H.M. Zabed, I. Khalil, M.R. Rahman, S.M. Islam, M.R. Karim, J. Uddin RSC Adv. **11**, 22937 (2021)
36. R. He, T. Kyu Macromolecules, 49 (15) 5637(2016)
37. A.P. V.Bocharova, A.P. Sokolov, Macromolecules **53**(11), 4141 (2020)
38. B.K. Money, K. Hariharan, J. Swenson, J. Phys. Chem. B **116**, 26, 7762 (2012)
39. J. Hu, W. Wang, R. Yu, M. Guo, C. He, X. Xie, ,H. Peng, Z. Xue RSC Adv. **7**, 54986 (2017). https://doi.org/10.1039/C7RA08471D
40. I. Dueramae, M. Okhawilai, P. Kasemsiri, H. Uyama Sci Rep **11**, 13268 (2021). https://doi.org/10.1038/s41598-021-92671-5
41. H.K. Koduru, Y.G. Marinov, S. Kaleemulla, P.M. Rafailov, G.B. Hadjichristov, N. Scaramuzza J Solid State Electrochem **25**, 2409 (2021). https://doi.org/10.1007/s10008-021-05018-5
42. K.K. Ganta, V.R. Jeedi, V.K. Katrapally, M. Yalla, L.N. Emmadi, J. Inorg. Organomet. Polym. **31**, 3430 (2021). https://doi.org/10.1007/s10904-021-01947-w
43. L. Xu, J. Li, W. Deng, L. Li, G. Zou, H. Hou, L. Huang, X. Ji Mater. Chem. Front. **5**, 1315 (2021). https://doi.org/10.1039/D0QM00541J
44. V. Kamboj, A. Arya, S. Tanwar, V. Kumar, A.L. Sharma Mater Sci. **56**, 6167 (2021). https://doi.org/10.1007/s10853-020-05667-3
45. S.S. Salehan, B.N. Nadirah, M.S. Saheed, W.Z. Yahya, M.F. Shukur, J. Polym. Res. **28**, 222 (2021). https://doi.org/10.1007/s10965-021-02586-y
46. S. Majumdar, P. Sen, R J. Ray Solid State Electrochem. **26**, 527 (2022). https://doi.org/10.1007/s10008-021-05093-8
47. S. Majumdar, P. Sen, R J. Ray Ionics **28**, 1403 (2022). https://doi.org/10.1007/s11581-021-04389-z
48. E. Sudaryanto, P.A.I.P. Yulianti, Conf. Proc. **1710** (1), 020003 (2016). https://doi.org/10.1063/1.4941464
49. P.A. Helen, K. Ajith, M.I. Diana, D. Lakshmi, P.C. Selvin, J. Mater. Sci: Mater. Electron. **33**, 3925 (2022). https://doi.org/10.1007/s10854-021-07587-7
50. P. Moni, J. Solid State Electrochem. **25**, 2371 (2021). https://doi.org/10.1007/s10008-021-05016-7
51. B.N. Choi, J.H. Yang, Y.S. Kim, C.H. Chung, RSC Adv. **9**(38), 21760 (2019). https://doi.org/10.1039/C9RA03555A
52. M.A. Ramli, M.I.N. Isa, J. Phys. Chem. B **120**(44), 11567 (2016). https://doi.org/10.1021/acs.jpcb.6b06068

Scheme

Scheme 1 is available in Supplementary Files section.

Figures

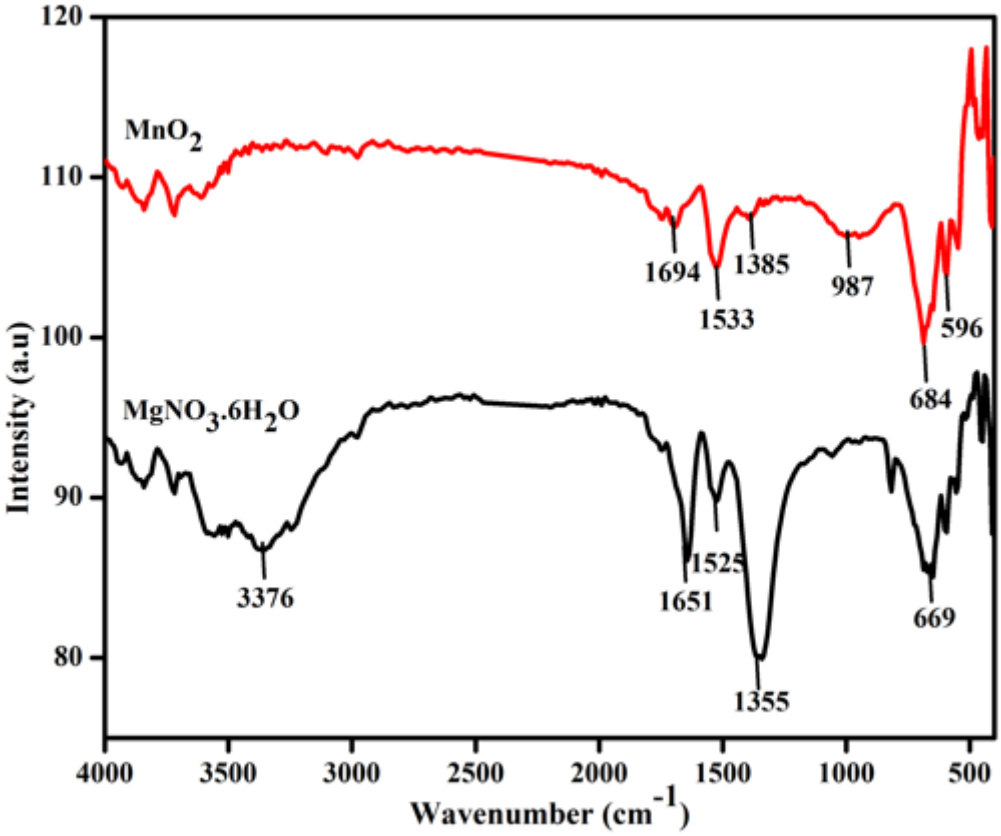

Figure 1

FTIR spectra of $MgNO_3.6H_2O$ (salt) and MnO_2 (filler)

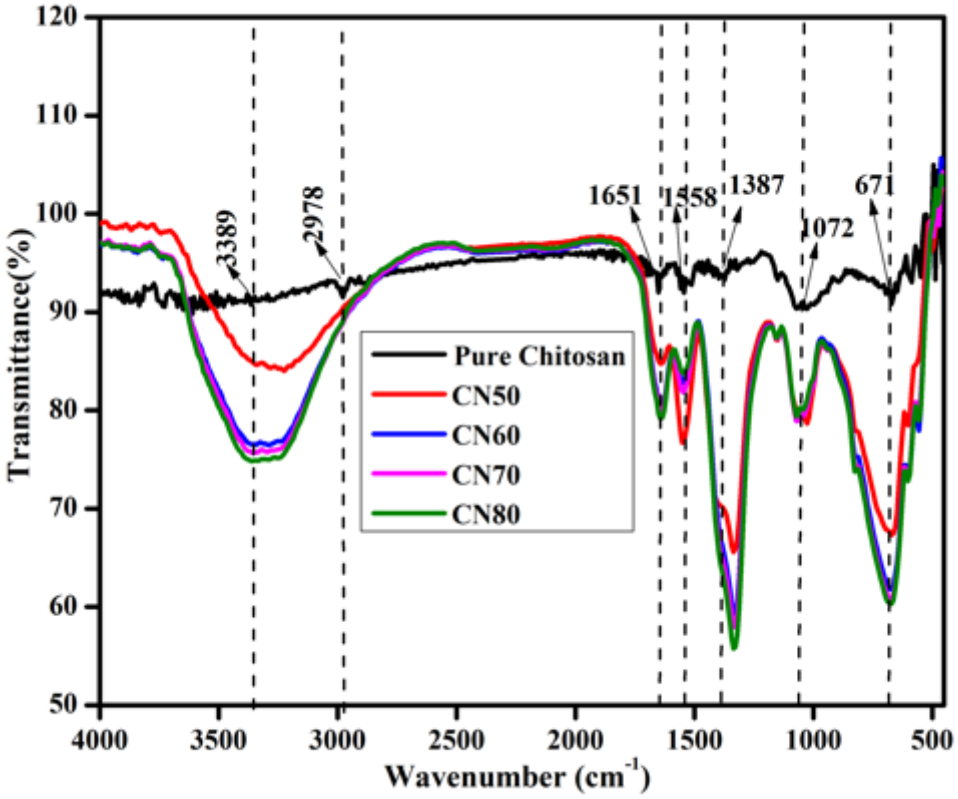

Figure 2

FTIR spectra of pure chitosan and chitosan with weight percentages of salt.

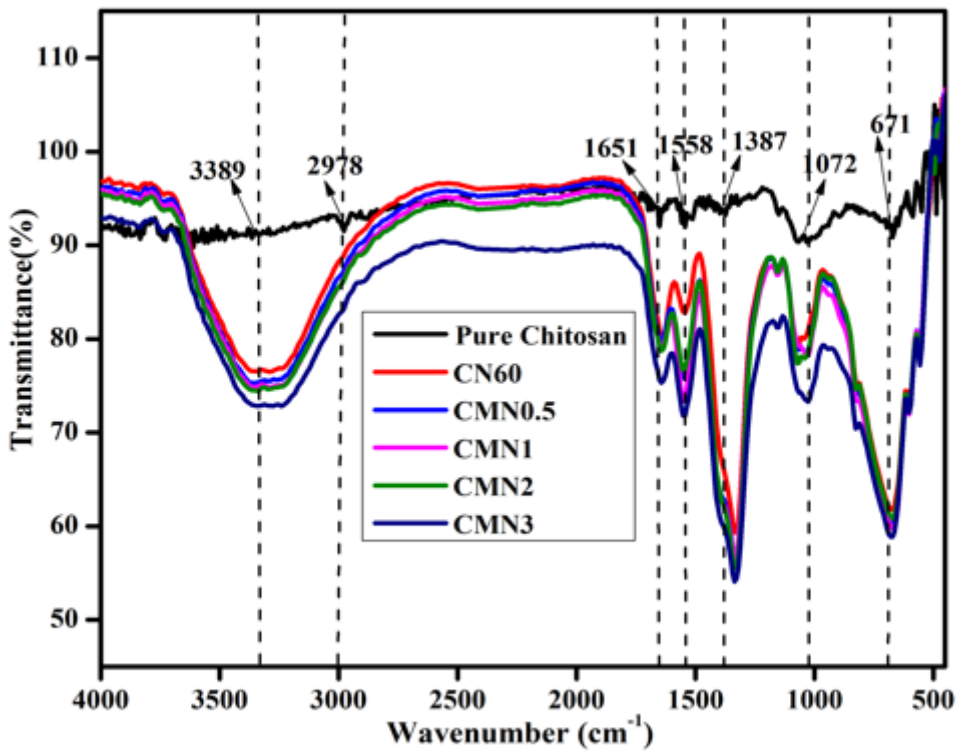

Figure 3

FTIR spectra of pure chitosan, chitosan with 60wt% of salt and filler in x wt% (0.5, 1, 2, 3)

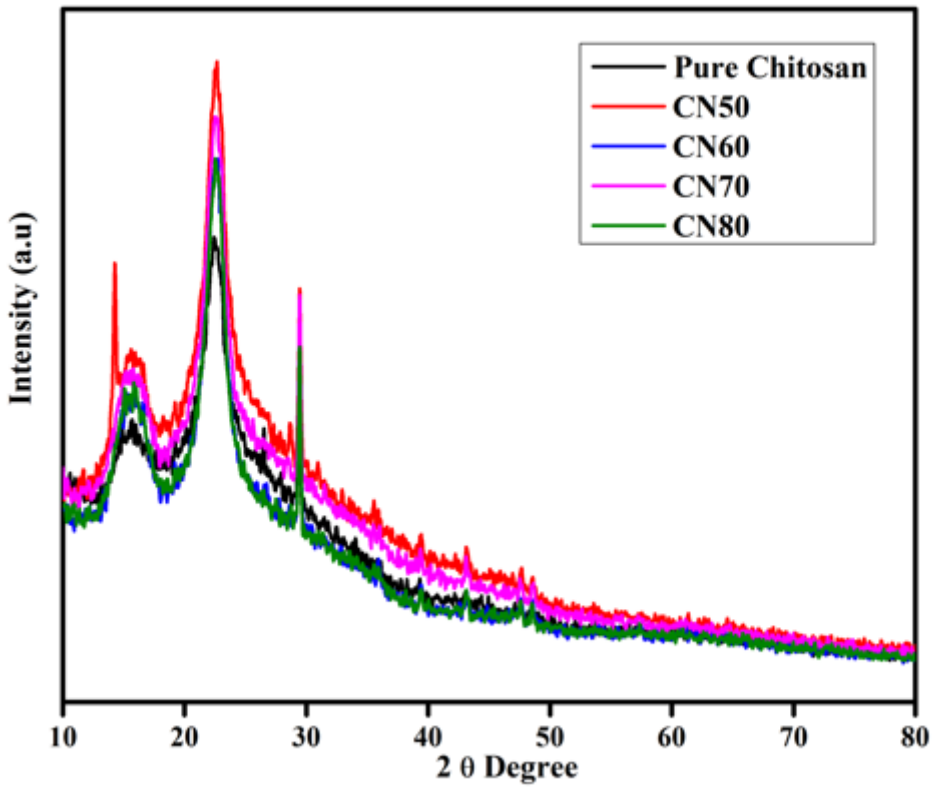

Figure 4

XRD pattern of pure chitosan and chitosan with different weight percentages of salt

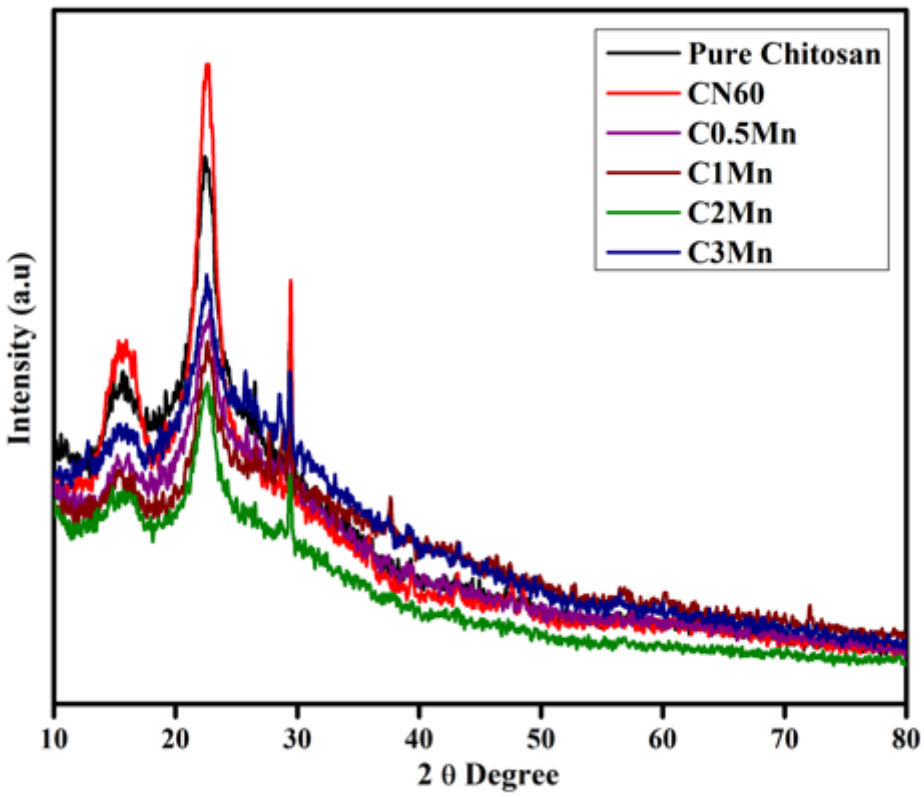

Figure 5

XRD pattern of pure chitosan, chitosan with 60 wt% of salt (CN60) and CN60 with different weight percentages of filler

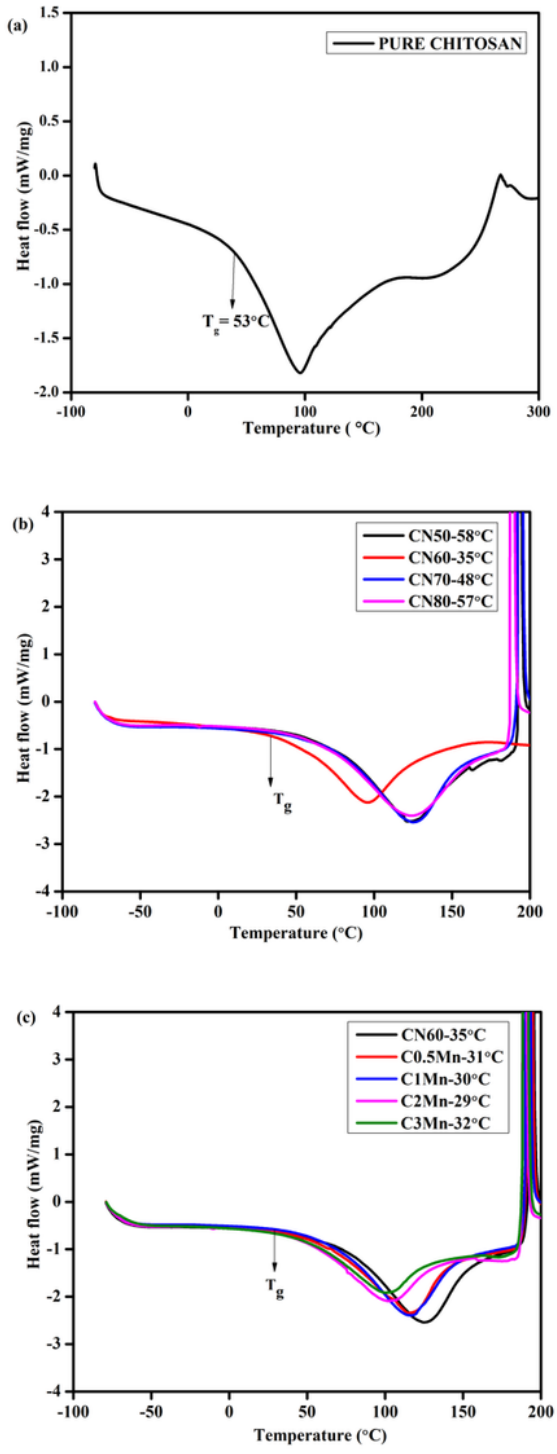

Figure 6

(a) DSC thermogram of pure chitosan, **(b)** chitosan with various amounts of salt content **(c)** chitosan with different amounts of filler.

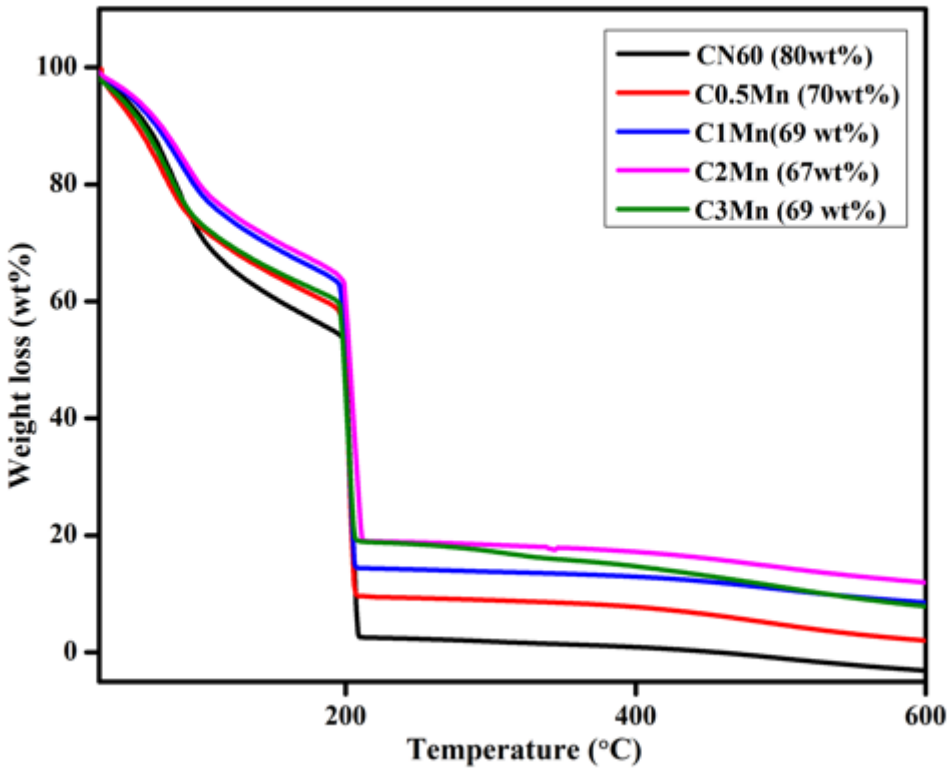

Figure 7

TG thermograms of CN60 and CN60 with different amounts of filler.

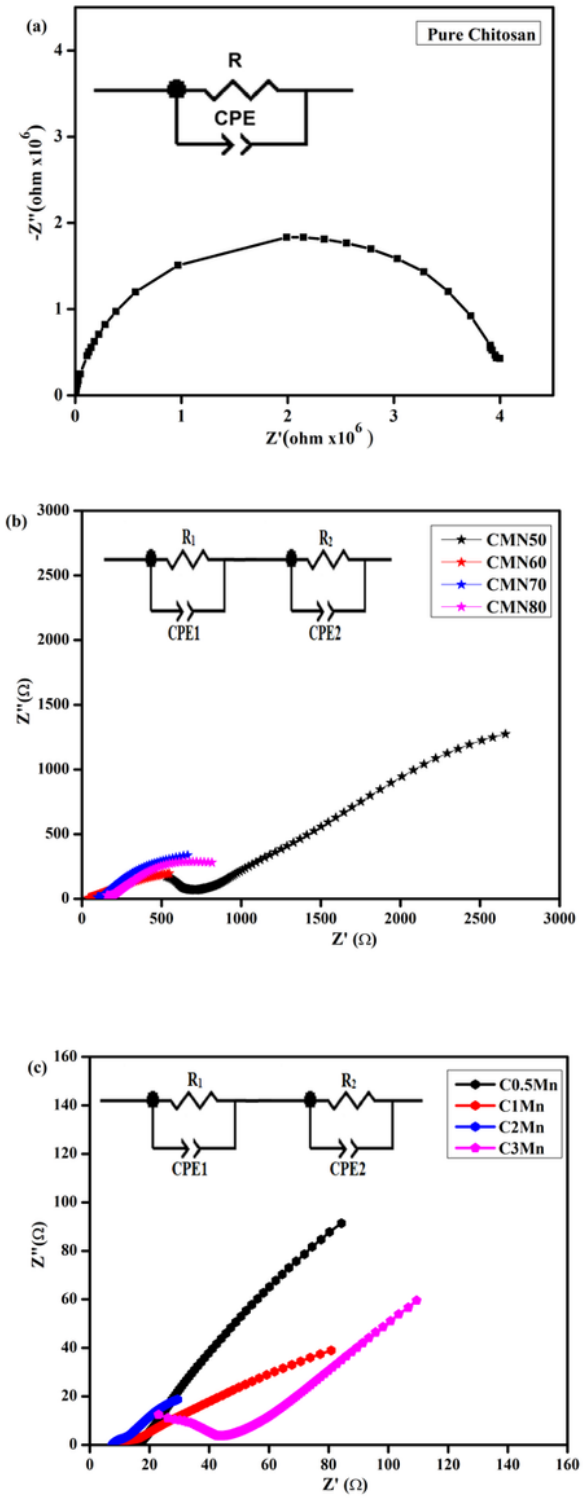

Figure 8

(a) Nyquists plot of pure chitosan **(b)** chitosan with salt in different weight percentages **(c)** chitosan with filler in different filler percentages

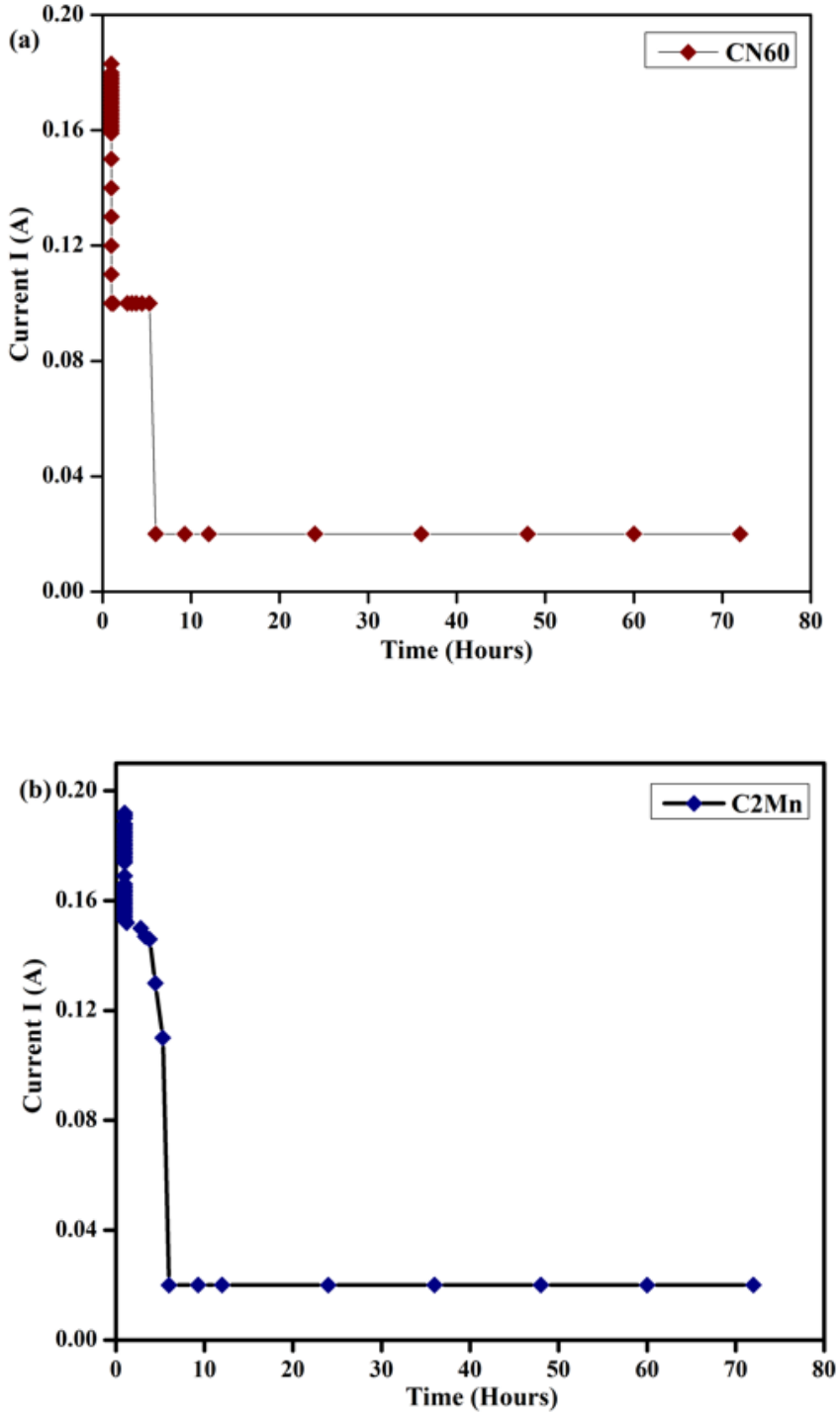

Figure 9

Transference number measurement of **(a)** CN60 and **(b)** C2Mn

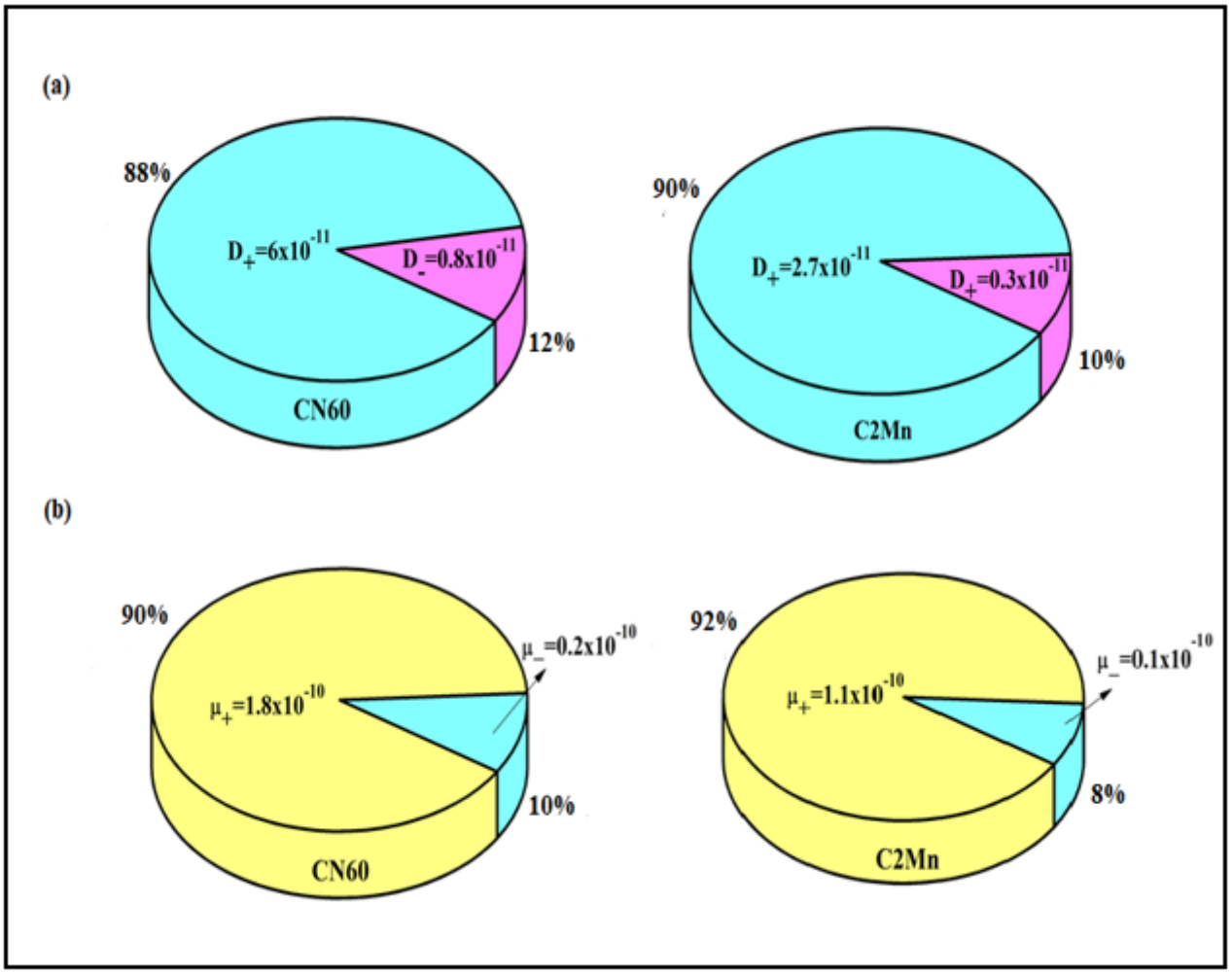

Figure 10

Pie chart depicting the individual contribution of cations and anions in transport parameters **(a)** mobility(μ) and **(b)** diffusion coefficient (D) process in electrolytes CN60 and C2Mn

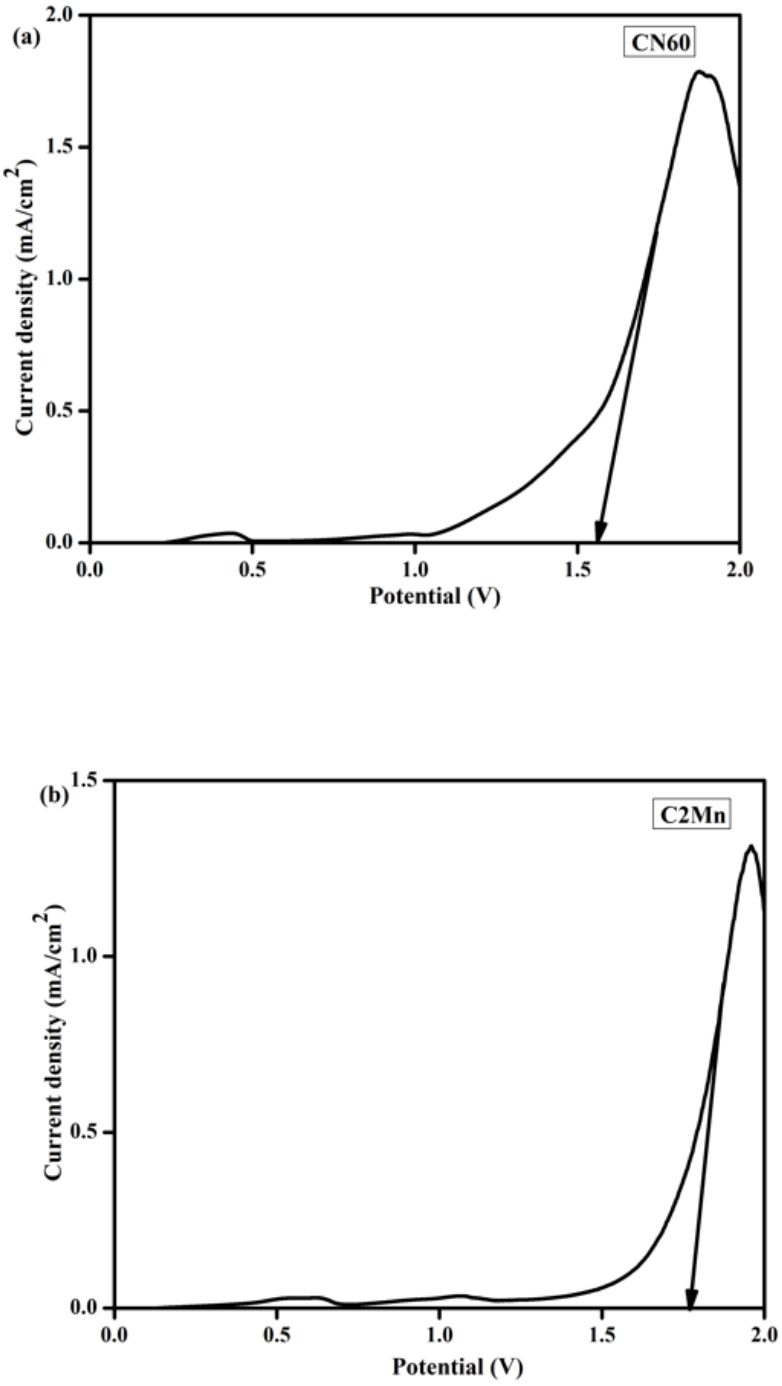

Figure 11

LSV analysis of **(a)** CN60 and **(b)** C2Mn

Supplementary Files

This is a list of supplementary files associated with this preprint. Click to download.

- Scheme1.png
- SI.docx